

Self-Assembly of Lecithin and Bile Salt in the Presence of Inorganic Salt in Water: Mesoscale Computer Simulation

Anastasia A. Markina,^{*,†} Viktor A. Ivanov,[†] Pavel V. Komarov,^{‡,§} Alexei R. Khokhlov,^{†,‡} and Shih-Huang Tung^{||}

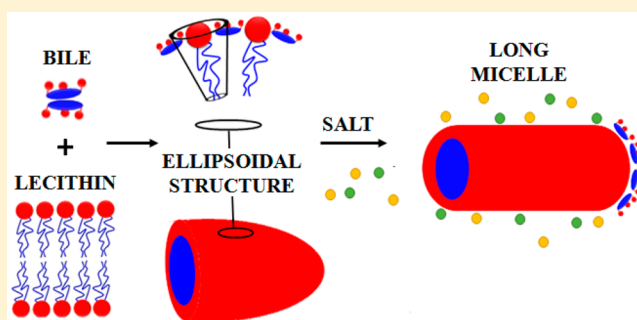
[†]Moscow State University, Moscow 119991, Russian Federation

[‡]Institute of Organoelement Compounds RAS, Moscow 119991, Russian Federation

[§]Tver State University, Tver 170100, Russian Federation

^{||}National Taiwan University, Taipei 10617, Taiwan

ABSTRACT: The influence of inorganic salt on the structure of lecithin/bile salt mixtures in aqueous solution is studied by means of dissipative particle dynamics simulations. We propose a coarse-grained model of phosphatidylcholine and two types of bile salts (sodium cholate and sodium deoxycholate) and also take into account the presence of low molecular weight salt. This model allows us to study the system on rather large time and length scales (up to about $\sim 20 \mu\text{s}$ and 50 nm) and to reveal mechanisms of experimentally observed increasing viscosity upon increasing the low molecular weight salt concentration in this system. We show that increasing the low molecular weight salt concentration induces the growth of cylinder-like micelles formed in lecithin/bile salt mixtures in water. These wormlike micelles can entangle into transient networks displaying perceptible viscoelastic properties. Computer simulation results are in good qualitative agreement with experimental observations.

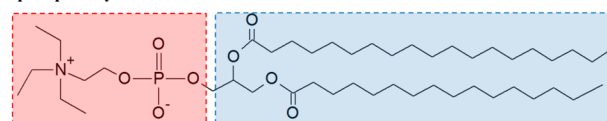


1. INTRODUCTION

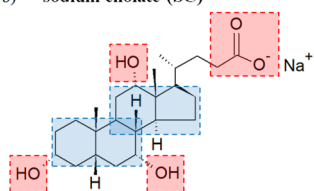
Self-assembling structures of biological surfactants can be used in manufacturing of composites with complex mesoscopic order, in developing of biodegradable materials, and in medical applications.^{1,2} There are two general classes of biological surfactants (phospholipids and bile salts) which play an important role in physiological processes. A typical representative of phospholipids is phosphatidylcholine (Figure 1a), a zwitterionic surfactant that has a positive charge on the choline group and negative on the phosphate group. It is insoluble in water and typically self-assembles into aggregates such as bilayers or vesicles. Bile salts belong to the class of steroids, and the presence of polar groups in the α -position leads to amphiphilic properties (Figure 1b). Bile salt molecules have the Janus-type disklike structure with hydrophobic and hydrophilic surfaces (so-called “facial amphiphiles”).^{3–5} Bile salt molecules generally form highly curved small micelles with an unusually low aggregation number (about 5–10) in water.^{3–9}

In the past, a large amount of experimental^{1–9} and theoretical^{10–20} work dedicated to systems containing lecithin has been done, including lecithin-based organogels and hydrogels (for review see refs 22 and 23 and references therein). The strong interest could be explained by biocompatibility, prevalence, and low cost of lecithin, which can be found in any living matter as a main component of the cell membrane, as well as the possibility to construct smart

a) phosphatidylcholine



b) sodium cholate (SC)



sodium deoxycholate (SDC)

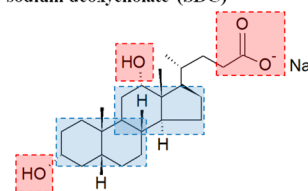


Figure 1. Molecular structures of (a) phosphatidylcholine and (b) sodium cholate (SC) and sodium deoxycholate (SDC). Hydrophilic and hydrophobic parts of the molecules are schematically marked by red and blue rectangles, respectively.

complex self-assembled morphologies.²⁴ In lecithin-based systems, aggregation morphology may be governed by bile salts^{22,23} or small polar molecules.^{25–29}

Received: May 11, 2017

Revised: July 22, 2017

Published: July 24, 2017

There are experimental studies^{4,27–29} dedicated to the interaction between ions and phospholipids in water. It was found that a bound ion facilitates denser packing of lipids and more extended conformation of their hydrophobic tails. The aggregation number of bile salt micelles in water increases with increasing ionic strength.²² Reducing the solubility of amphiphilic molecules (e.g., bile salts) can be explained by a number of reasons:^{30–32} (1) dissociation of an inorganic salt makes the bile salt dissociation less favorable due to the entropic reasons, and nondissociating salts (and acids) are poorly soluble in water;²² (2) hydrophobicity of the nonpolar parts increases; (3) electrostatic repulsion between charged groups decreases by screening, therefore they can come closer to each other and join together to form larger aggregates; and (4) hydrogen bonds between small electronegative atoms (O or N) of surfactant molecules and water are destroyed. Effective interactions between surfactant molecules with charged groups depend not only on the concentration of salt but also on the type of ions. Ions of certain salts can improve the solubility of some compounds.^{30,31} Specific ion effects influence self-assembling processes of polyelectrolytes (e.g., strong ion specificity is observed for sodium acetate and sodium chloride in chitosan aqueous solutions).³²

Despite a large amount of progress, theoretical and computer simulation studies^{10–20} still do not cover all properties and self-assembling details of such systems. In this study, we are focused on the computer simulation study of morphologies of lecithin micelles in aqueous solution where both bile salt and inorganic salt play the key role of gelation agents. We describe micellar size and shape, as well as mechanisms of micellar growth. To the best of our knowledge, computer simulation study of such systems (aqueous solutions of lecithin and bile salts in the presence of low molecular weight salt) has not been performed previously.

During the last decades, several theoretical and simulation studies investigating lecithin and bile salt systems have been published.^{14–20} Many of these computer simulation studies were based on coarse-grained (CG) models of lipids and applied well-known force-fields (e.g., the MARTINI force-field).¹⁴ Related CG bile salt models can also be found in the literature.^{15–18} These models have been recently used for studying association behavior of bile salt/lipid aqueous solutions, for investigation of size, composition, and shape of the micelles, and the transition kinetics from vesicles to mixed micelles.^{19,20} In ref 20, it has been shown that depending on the number of lecithin molecules, either vesicles or discs can be formed and that adding bile salt solubilizes lecithin vesicles and bilayers. In all above-mentioned computer simulation studies, solvent-free models have been used, and the effect of adding inorganic salt has not been studied. Moreover, in previous simulations, the size of system was rather small (i.e., it was possible to investigate a single large micelle or a few small micelles on rather small times, even for CG models used so far).

We have tried to overcome the disadvantages of previous works, which were quite limited in scale and time of modeling and cannot completely represent behavior of the studied systems. In order to be able to simulate a system containing many micelles and to obtain an equilibrium size distribution (i.e., in order to increase the length and time scales in simulation), one needs to go to «more coarse-grained» models trying to keep the most important features of the real systems, and for this goal DPD method seems to be well

suitable for such systems and such phenomena.²¹ CG models are highly sensitive to the parameters of interaction, the choice of coarse-graining, etc. At the same time, such models can demonstrate key features in the behavior of such systems, which is interesting both for fundamental and practical applications (e.g., for targeted design of real prototypes of model objects). Of course, as at any coarse-graining, some features of a system can be lost, but a CG model can still keep the most crucial features of a system under study. In this paper, we ask the question whether it is possible to make a «more coarse-grained» model for lecithin/bile salt aqueous solutions which will be able to keep the essential physics. Advantage of our model and DPD method is the fast equilibration on long times and large scales (due to soft potentials, a large time step can be used). Such models are good for simulation of initial stages of phase formation, and later a more detailed atomistic representation with appropriate force field can be restored for the systems using a reverse mapping procedure. Starting from a random configuration, we will be able to reach the equilibrium state very fast.

As regards to the coarse-graining itself (i.e., the substitution of groups of atoms in the atomistic model by a particle in the CG model), our CG model is quite similar to the model used, for example, in ref 14, however, the «grains» in our model are even slightly larger. Our model represents the molecular geometry of lecithin and bile salts reasonably well to be able to reproduce experimental results. The main advantage of our model is the large time step due to soft potentials that allow us to investigate the systems on about two orders of magnitude times longer than in previous studies. We have taken the solvent (water) explicitly into account, but we have implicit low molecular weight salt in our model. However, our model for implicit inorganic salt allows us to reproduce rather well the experimental results (e.g., the viscosity increasing due to growing of micelles in lecithin/bile salt aqueous solutions upon adding inorganic salt).

Experimental rheological study²² shows the increase of viscosity in lecithin/bile salt water solution upon increasing the inorganic salt concentration, and thus phenomenon was assumed to be related to the growth of lecithin/bile salt micelles into long flexible wormlike structures²² followed by their entanglement into transient networks. It was shown that micellar growth requires a sufficient amount of inorganic salt (for example, NaCl) which serves to “salt out” the amphiphiles.²² The zero-shear viscosity of the lecithin/bile salt mixture in water was studied²² as a function of the molar ratio of bile salt to lecithin (B_0) and inorganic salt concentration. At low ionic strength, the solution has low viscosity, while viscosity increases significantly upon adding inorganic salt. And finally, when salt concentration is sufficiently large, the phase separation in two coexisting liquid phases takes place. A qualitative explanation of observed phenomena was given in ref 22; however, the question about molecular mechanisms of formation of wormlike micelles still remains open. We have previously reported our computer simulation study of the effect of adding bile salt to lecithin organosols³³ and compared our results with experimental data.¹⁵ In this paper, we study aqueous solutions of lecithin/bile salt mixtures and are focusing mainly on the ionic strength impact.

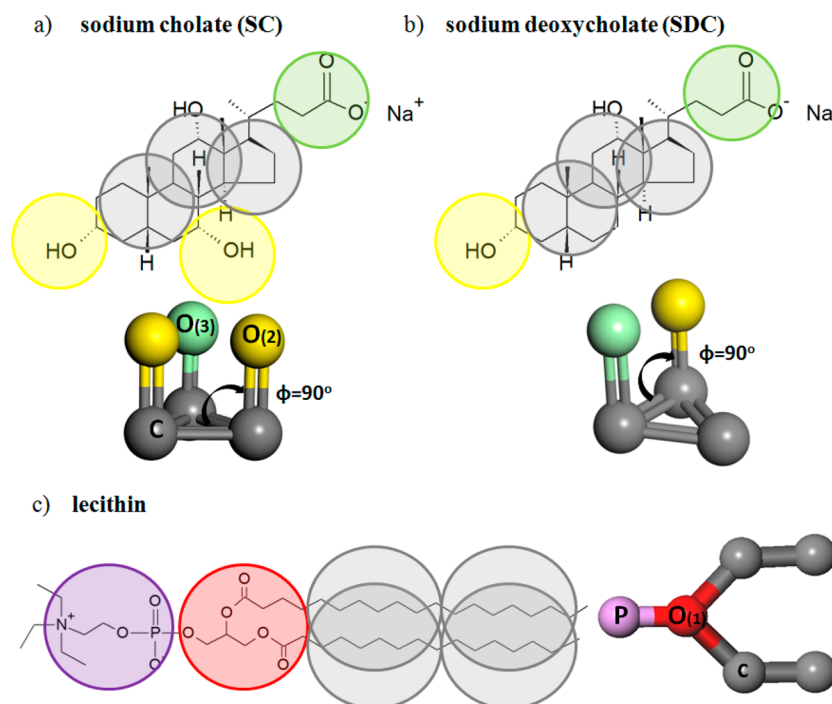


Figure 2. CG model of (a) bile salts SC, (b) SDC, and (c) lecithin. Preferred bending angles Φ for hydrophilic parts of bile salt are shown by arrows. Hydrophilic parts of bile salts are marked as yellow O(2) and green O(3), and as purple P and red O(1) for lecithin. Hydrophobic parts of both surfactants are colored by gray C. This color scheme and subsystem symbols are used in all figures below.

2. MODEL AND SIMULATION TECHNIQUE

Computer simulations of lecithin/bile salt mixtures has been performed in the framework of the dissipative particle dynamic (DPD) in canonical (NVT) ensemble for systems consisting of the following molecules (see Figure 1): (1) lecithin (phosphatidylcholine); (2) bile salts: sodium cholate (SC) and sodium deoxycholate (SDC); (3) water; and (4) low-molecular weight salt (can be NaCl, for example), which was implicitly taken into account.

The DPD is the mesoscopic computer simulation method widely used for studying structural properties of aqueous solutions, colloidal dispersions, as well as polymer melts and solutions.^{34,35} The DPD method utilizes CG models and “soft” potentials of intermolecular interactions and that allows selecting a sufficiently large time step in a finite-difference scheme for Newton equations of motion

$$m_j \ddot{\mathbf{r}} = \mathbf{f}_j$$

and enables studying of molecular systems on larger spatial (up to microns) and time (up to milliseconds) scales as compared to the atomistic molecular dynamics. Each DPD-particle (all having diameter $\sigma = 1$ and mass $m = 1$ in arbitrary units) is associated with a group of small molecules, some fragments of macromolecules, or with a statistical segment (Kuhn segment of a polymer chain). The characteristic time unit τ is $\sigma \sqrt{m/k_B T}$ (k_B is the Boltzmann constant and T the absolute temperature). Integration of the system of equations of motion was realized using the Verle method with a time step $\Delta t = 0.05 \tau$. The net force applied to each particle consists of five terms:

$$\mathbf{f}_j = \sum_{i \neq j} (\mathbf{F}_{ij}^b + \mathbf{F}_{ij}^a + \mathbf{F}_{ij}^c + \mathbf{F}_{ij}^d + \mathbf{F}_{ij}^r)$$

where the summation is performed over all particles within the cutoff radius r_c . The first two forces are the spring force (F_{ij}^b), which takes into account the covalent bonds between adjacent CG particles in molecules, and the elastic force of bond angle deformation (F_{ij}^a) is used to take into account the intramolecular stiffness.³³ Both forces are linear on deviation from the equilibrium bond length $l_0 = \sigma$ and the equilibrium bond angle Φ_0 , respectively, and the stiffness parameters were taken from our previous work.³³ Preferred bond angles $\Phi_0 = 90^\circ$ for hydrophilic parts of bile salts are shown by arrows in Figure 2, while there is no bending potential applied to angles between other bonds. The conservative force (F_{ij}^c) is the soft-core repulsion between particles i and j :

$$\mathbf{F}_{ij}^c = \begin{cases} a_{ij}(1 - r_{ij})\hat{\mathbf{r}}_{ij}, & r_{ij} < \sigma \\ 0, & r_{ij} > \sigma \end{cases}$$

$$\hat{\mathbf{r}}_{ij} = \mathbf{r}_{ij}/r_{ij}$$

where a_{ij} is the maximum repulsion force between beads i and j . The remaining two forces are the dissipative force (F_{ij}^d) which takes into account the friction of an effective medium and the random force (F_{ij}^r) which describes the thermal motion of the system. The values of coefficients were taken from refs 34 and 35. The system density was chosen to be equal to $\rho = 3\sigma^3$ for correct description of the water isothermal compressibility.³⁵ For this density value, the parameter a_{ij} can be expressed in terms of the Flory–Huggins parameter as $a_{ij} = 25 + 3.27\chi_{ij}$. The Flory–Huggins parameter describes the volume interaction between species α and β and depends on the Hildebrand solubility^{36,37} parameter δ :

$$\chi_{\alpha\beta} = \frac{V_{\text{ref}}(\delta_\alpha - \delta_\beta)^2}{RT} - \chi_S$$

where R is the gas constant, V_{ref} is the average molar volume of CG particles, and its value is equal to $142 \text{ cm}^3/\text{mol}$ for our CG model (see below), χ_s is the entropic contribution to the mixing free energy; usually $\chi_s \sim 0$ and can be omitted. In accordance with the Hildebrand theory, mutual solubility of nonelectrolytes increases with decreasing the difference between their solubility parameters.^{36,37} The Hildebrand solubility parameter is the square root of the cohesive energy density:

$$\delta = \sqrt{\frac{\Delta H_v - RT}{V_m}}$$

where V_m is the molar volume in the condensed phase and ΔH_v is the heat of vaporization.

To simulate lecithin/bile salt mixtures in aqueous solution in the frame of DPD method, we have improved our CG model³³ shown in Figure 2. The symbols for CG particles and corresponding fragments are marked with different colors in Figure 2, and this color scheme will be used in the snapshots of the system below. When choosing the fragments of molecules and assigning them to different beads (particles of different types), it was important to take into account the proportion of sizes of lecithin and bile salt molecules, as well as structural features of the bile salt molecule, namely its geometrical peculiarities (planar Janus-type structure). In accordance with our CG schema, the diameter of one DPD particle corresponds to 7 \AA . In this case, one DPD particle corresponds to eight water molecules.

CG representation for bile salt looks like a “backless stool”, whose three or two legs [composed of hydrophilic groups O(2) and O(3)] are connected to hydrophobic skeleton and fixed by introducing the potential on the valence angles and choosing $\Phi_0 = 90^\circ$. Both lecithin charged groups, choline and phosphate, were combined into a single CG polar particle P to maintain the correct balance between the size of polar and nonpolar groups. In general, the charged groups affect the formation of the double layer structure but only at short distances. Indeed, in the aqueous solution, the Bjerrum length is $\sim 6.9 \text{ \AA}$ at $T = 300 \text{ K}$. This value is comparable to the DPD particle size. Since the particle P can be considered as a dipole with a shoulder length of $\sim 4.9 \text{ \AA}$, the energy of the Coulomb interaction of two such particles exceeds the energy of thermal motion only at small distances, when they can already bind due to the intermolecular interaction. In our model, only their polar nature is taken into account [i.e., how do they interact with water (high hydrophilicity)].

Five different CG schemes including models of lecithin from refs 33, 38, and 39 have been tested before we have found an appropriate model which reproduces formation of micelles. Our CG model does not include specific interactions like hydrogen bonding but only purely hydrophobic–hydrophilic interactions, and the key part of the model is a specific geometry of molecules.³³ Previous simulations³³ with using similar CG scheme for lecithin/bile salt in organic solvent show that micellar morphology and aggregation number are in qualitative agreement with experimental data.²³

In this paper, we suggest a method to implicitly take into account the low-molecular weight salt in computer simulations. Small amount of inorganic salt reduces the number of hydrogen bonds between the lecithin and water (affinity of the polar groups to water), which reduces the solubility of polar groups.^{40–42} Following ideas from ref 43, we propose to describe the presence of inorganic salt in an aqueous solution

by decreasing Hildebrand solubility parameter of polar groups δ_p of lecithin and bile salt, whereas the solubility parameter of water δ_w remains unchanged. The new values of solubility parameters for polar groups P, O(1), O(2), O(3) are calculated as $(1 - C)\delta_p$, where the parameter $C \in [0; 0.25]$. The value $C = 0$ indicates the absence of inorganic salt, increasing of C means reduction of solubility parameter δ_p and reflects the presence of inorganic salt in the solution. We have performed simulation for different values of C , while Figures 5–8 show data only for high $C_2 = 0.2$ ($\sim 6 \text{ M NaCl}$) and moderate $C_1 = 0.15$ ($\sim 4.5 \text{ M NaCl}$) salt concentration. The model takes into account positively charged ions formed during the dissociation of bile salt and both positively and negatively charged ions due to the addition of inorganic salt. At the temperature $T = 300 \text{ K}$ chosen in our modeling, the ions are distributed in the solution volume uniformly¹⁴ as the temperature is above the Manning threshold.⁴⁴ An estimate of the Debye radius (lecithin 100 mM , bile salt 90 mM , and NaCl $0.15\text{--}1\text{M}$) gives values of $\sim 6.2\text{--}2.9 \text{ \AA}$ that allow us to conclude that at long distances all electrostatic interactions are completely screened. In the course of the verification of our CG model, we have studied the effect of internal rigidity on the type of formed structures. We do not observe significant difference in formed structures by varying the stiffness and the equilibrium length between beads (parameters of spring force).

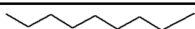
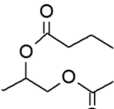
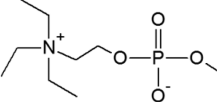
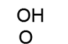
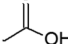
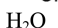
Summarizing, we would like to mention here limitations of our CG model. First, it does not properly reflect the size of molecular groups (e.g., equal O(2) and C beads in CG representation originally have difference size in atomistic representation). However, the total ratio between linear sizes of lecithin and bile salt molecules (2:1) is kept correctly: although one molecule of lecithin and one molecule of bile salt consist of 6 C beads, their linear size is different due to a “backless stool” structure of bile salt against the two-tail structure of lecithin. Second, our CG model is not able to take into account hydrogen bonding interactions; so, for example, we cannot observe the formation of secondary micelles in the bile salt solution.⁴⁵

The Askadskii semiempirical method⁴⁶ was utilized to calculate the solubility parameters and volumes of molecular fragments, which correspond to the CG particles P, O(1), O(2), O(3), C, and W (for water). The obtained values of solubility parameters have been checked by means of the atomistic molecular dynamics with using the PCFF force field,⁴⁷ which we have already used to study other systems,⁴⁸ and a very good coincidence has been obtained for all particles except P and O(3). For these two CG particles, we cannot trust the values given by the Askadskii method because this method does not take into account the contribution of electrostatic interactions to the total energy of a system, and we have used the values obtained from the atomistic molecular dynamics. The characteristics of molecular fragments are presented in Table 1.

Finally, we would like to emphasize that the only difference between SC and SDC molecules is the presence of two O(2) groups in SC molecule, instead of one such group in SDC molecule. The CG model for SDC is almost the same as SC but includes only one O(2) bead instead of two. Therefore, total number of hydrophilic beads in the CG model for SDC is two (see Table 1 for details of chemical structure of molecular fragments).

The simulation cell of the size $60 \times 60 \times 60 \sigma^3$ containing 648 000 ($\sim 10^6$) particles was used for all simulations. To

Table 1. Subsystems Symbols, Chemical Structure of Molecular Fragments, and Their Hildebrand Solubility Parameter δ

Subsystem	Structure	$[\delta] = \left(\frac{J}{\text{cm}^3}\right)^{\frac{1}{2}}$
C		16.3
O(1)		21.2
P		39.4
O(2)		41.0
O(3)		41.0
W		42.0

control the system equilibration process, we monitored the system energy and the micelle size distribution. Typically, these observables did not vary with time after about 0.5 million simulation steps, and this was for us the criteria that the system has reached equilibrium. The total simulation time was about 1.5–2 million simulation steps to accumulate statistics at equilibrium and to perform an averaging of time series, and an additional averaging has been performed over three independent simulation runs.

It should be noted that the selected coarse scale gives us the following estimates for real scales and time intervals, namely, the selected simulation cell size corresponds to a volume of $420 \times 420 \times 420 \text{ \AA}^3$, and according to ref 49, $\Delta t \sim 41 \text{ ps}$ or the total duration of the productive run is $20.5 \mu\text{s}$ in the case of 500000 Δt steps that is difficult to achieve when using atomistic simulations.

3. RESULTS AND DISCUSSION

3.1. Morphological Changes upon Adding Inorganic Salt. Bile salt molecules have a hydrophobic and a hydrophilic surface and form in aqueous solutions micelles with low aggregation number, while phospholipids generally tend to form vesicles or bilayers in water (see Figure 3a). Figure 3 shows characteristic morphologies observed in aqueous solution of pure lecithin and SC upon adding inorganic salt. Without inorganic salt, bile salt tends to form micelles with low aggregation number about 5–6 in aqueous solution (see Figure 3a), and this data is in agreement with refs 3–9 and 17. Addition of inorganic salt induces the growth of short oblate beltlike structures due to reducing solubility leading to reducing the surface of all micelles and due to the planar Janus-type structure of bile salt molecules. The quasi-two-dimensional beltlike structures grow because of parallel orientation of bile salt molecules, which place their hydrophobic groups in the micelle core. However, we do not observe significant increase in micelle length (i.e., formation of wormlike micelles), in the pure bile salt aqueous solution upon adding inorganic salt. For pure lecithin solution, we observe vesicles both in the absence and in the presence of inorganic salt (Figure 3).

Phosphatidylcholine and bile salt in aqueous solution are assembled in rather short-ellipsoidal micelles (see Figure 4). Addition of low molecular weight salt leads to an increase in viscosity due to growing of long wormlike micelles, which form entanglements, as was assumed in ref 14. There are two main factors affecting the viscosity of such solutions:⁵⁰ the effective length of micelles (L) and the volume fraction of surfactant (φ), and the viscosity is determined as $\eta_0 \sim L^3 \varphi^{15/4}$ (see ref 50). The growth of elongated structures leads to their entanglement and formation of a dynamic network accompanied by viscosity increase. The presence of small ellipsoidal micelles as well as branched cylinders leads to the viscosity reduction. The amount of surfactant was fixed in simulation; the volume fraction of lecithin and bile salt was equal to $\varphi_0 = 0.005$ (number of molecules is 5400 for each), that is equivalent to lecithin concentration of about 100 mM and bile salt concentration of about 90 mM. The molar ratio of bile salt to

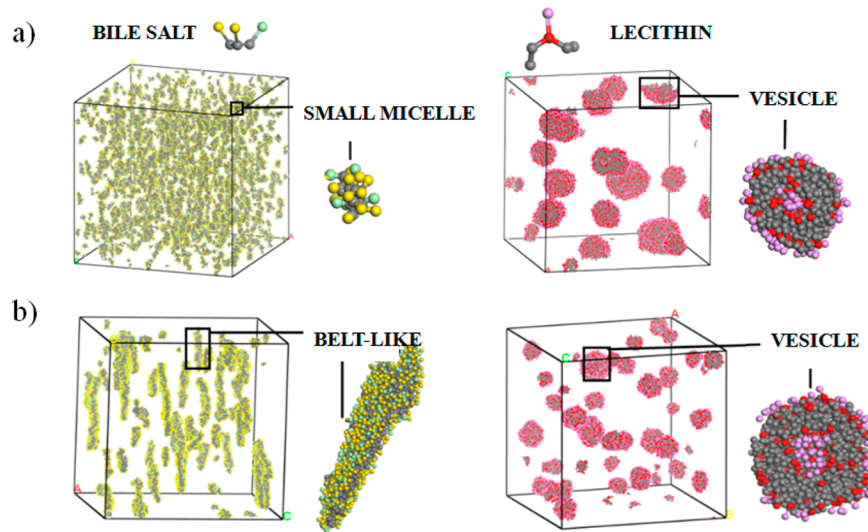


Figure 3. Morphological changes in aqueous solutions of the SC (on the left) and lecithin (on the right) upon adding inorganic salt: (a) system without salt and (b) in the presence of inorganic salt with concentration C_2 , the volume fraction of surfactant in both cases $\varphi_0 = 0.05$. The solvent particles are not shown.

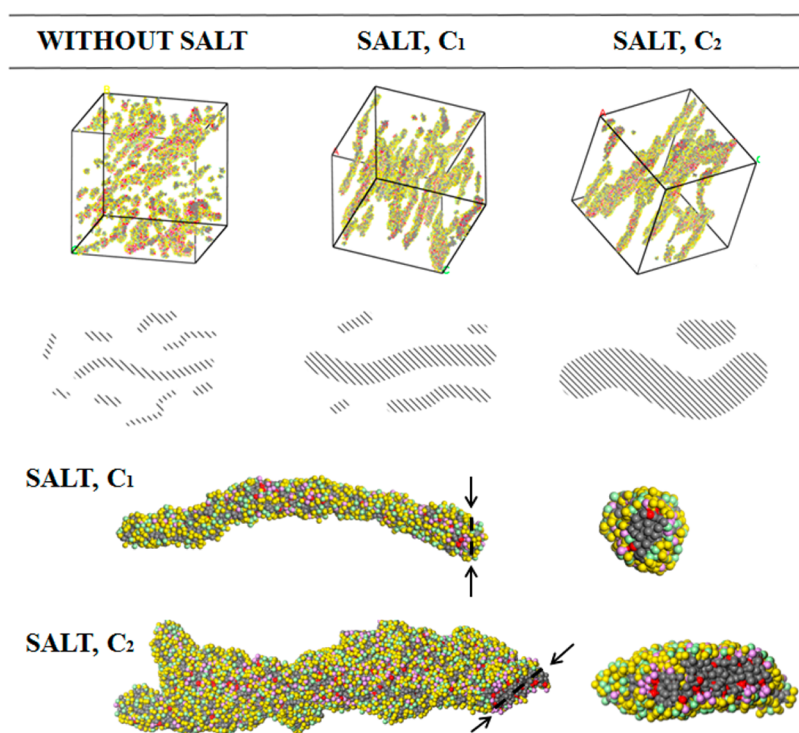


Figure 4. Structures formed in aqueous solutions of lecithin/bile salt SC with inorganic salt. From the left to the right: systems without salt ($C = 0$) and in the presence of inorganic salt (with concentrations C_1 , C_2). Dashed lines schematically show micelles.

lecithin was $B_0 = 0.9$, and the total volume fraction of all components, including the solvent, was equal to unity.

Figure 4 shows the behavior of SC-lecithin mixture in aqueous solution in the presence of low-molecular weight salt. In the absence of inorganic salt, we observe formation of a large amount of rather short thin micelles. Increasing inorganic salt concentration leads to reducing the number of micelles accompanied by increasing their thickness and length. The driving force of aggregation of small micelles is the decreasing of solubility of polar groups in water. Typical micelles' shapes are shown at the bottom of Figure 4. Upon increasing inorganic salt concentration ($C_2 > C_1$), micelles become thicker and flatter. Adding of inorganic salt reduces the solubility of micelles due to decreasing of hydrophilicity of polar parts of surfactants (because of destroying hydrogen bonds between electronegative atoms and water molecules⁴²). Aggregation of micelles becomes favorable, but due to peculiarities of molecular structures of lecithin and bile salts, the decreasing of the number of contacts between surface and solvent is realized by means of formation of elongated micelles (which can be confirmed by simple geometric considerations^{22,23,33}).

3.2. Cluster Analysis. We have performed the cluster analysis for specified particles to study the number of beads per micelle.^{33,51} All calculations were carried out for C beads; the cutoff radius was set $r_c = \sigma$. The beads C correspond to the hydrophobic part of the lecithin and are located in the cores of micelles, therefore such choice of the cutoff radius allows us to distinguish two closely located micelles as separate clusters.³³ We have tested several other values of the cutoff radius $r_c < 1.4 \sigma$, but we have not observed any significant difference in the results of cluster analysis.

The histogram in Figure 5 is based on results of cluster analysis and shows the volume fraction of micelles versus the number of particles per micelle (aggregation number) in the

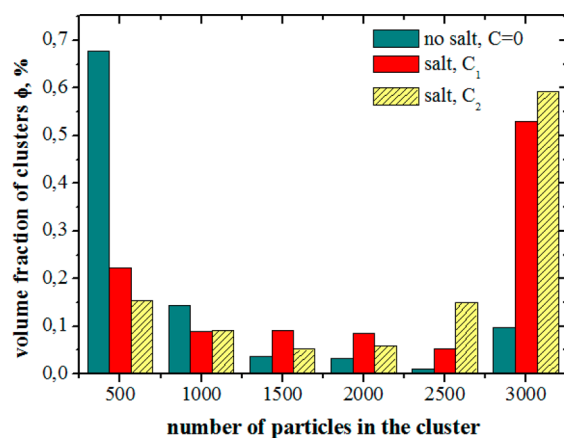


Figure 5. Volume fraction of beads in clusters versus the number of beads per cluster (aggregation number) for systems without salt ($C = 0$) and in the presence of inorganic salt (C_1 , C_2). Cyan bars correspond to $C = 0$, red bars to C_1 and yellow bars to C_2 . Here, and in Figures 6–8 below, the data are for bile salt SC.

system. The first bar contains all clusters with amount of particles (C beads) less than 500, the last bar contains all clusters with amount of particles more than 3000. For large salt concentration C_2 we observe clusters consisting of up to 9000 particles. Volume fraction of clusters is calculated as the number of particles in a cluster divided by the total number of surfactant particles (i.e., the total number of beads both in lecithin and in bile salt molecules). Addition of inorganic salt increases the volume fraction of long micelles and reduces the percentage of short micelles in the system. For C_1 and C_2 , the main peak on the histogram is shifted toward the higher number of particles in the cluster (from 500 to 3000), and

clusters with a large number of particles have higher volume fraction (most molecules are concentrated in large clusters).

3.3. Shape of Micelles. In order to analyze the form of growing micelles, one can use the method^{52,53} based on calculation of the shape parameters $K_1 = (\lambda_3 + \lambda_2)/(\lambda_1 + \lambda_2)$ and $K_2 = (\lambda_3 + \lambda_1)/(\lambda_1 + \lambda_2)$, where $\lambda_1, \lambda_2, \lambda_3$ are three eigenvalues of the gyration tensor of each micelle sorted in descending order [$\lambda_1 = \max(\lambda_x, \lambda_y, \lambda_z)$, $\lambda_3 = \min(\lambda_x, \lambda_y, \lambda_z)$]. The sum of these parameters $\lambda_1 + \lambda_2 + \lambda_3$ is equal to the squared gyration radius R_g^2 . The placement of the ideal rod on the (K_1, K_2) -plane is the point (0, 1), the ideal disk is located at (0.5, 0.5), and the ideal sphere at (1, 1). Figure 6 displays the

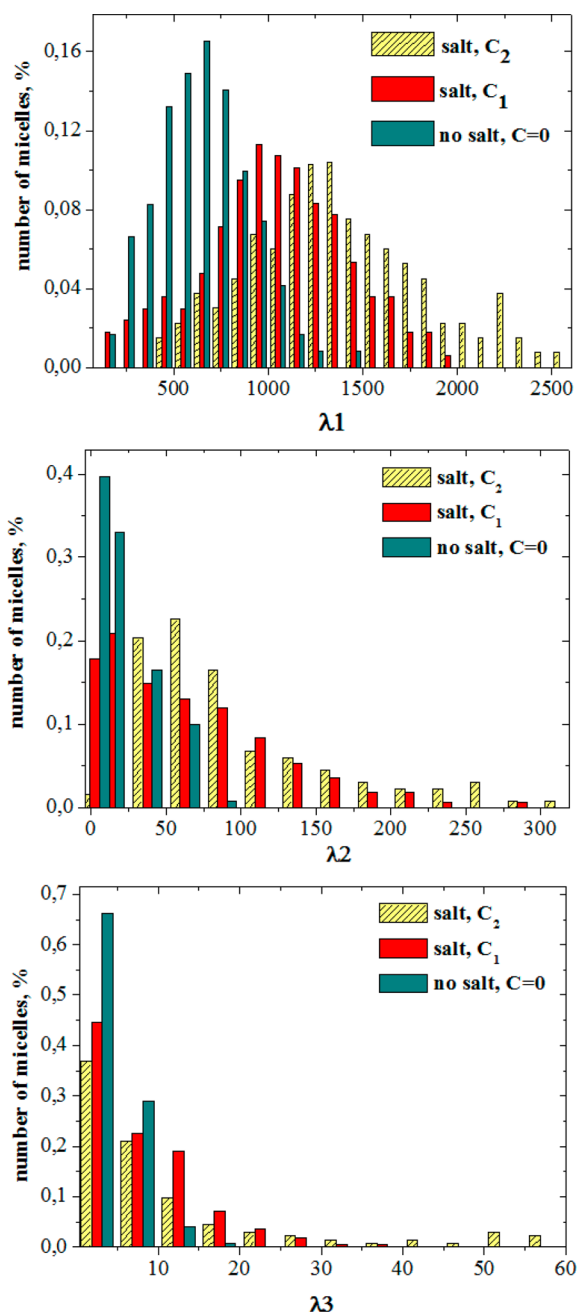


Figure 6. Histogram of the eigenvalues of the gyration tensor of micelles having the number of particles $N > 300$ without salt ($C = 0$) and in the presence of inorganic salt (C_1, C_2). Cyan bars correspond to $C = 0$, red bars to C_1 , and yellow bars to C_2 .

histogram of eigenvalues of the gyration tensor for the clusters, which have the number of particles $N > 300$. We chose only clusters with $N > 300$ to monitor cluster growth (because small clusters could be a result of inaccuracy of cluster analysis method or just small aggregates of bile salts). For both systems with salt (with concentration C_2 and C_1), the main peak is located at larger λ_1 values in comparison to $C = 0$. The distribution for C_2 is wider than that for C_1 and is shifted toward larger λ_1 values (i.e., the addition of inorganic salt induces the growth of λ_1). For systems with C_1 and $C = 0$, λ_2 values are very close, for C_2 the position of main peak is a little bit shifted. For λ_3 , we observe almost the same distributions for all three systems. This may correspond to the micelle growth upon adding inorganic salt and predominance of more asymmetrical and elongated structures in the system with C_2 .

In Figure 7, we show our results as two-dimensional histograms of K_1 and K_2 parameters for systems with salt and without salt for clusters having the number of particles $N > 300$. The distribution for system without salt is very narrow, the peak is located very close to the point (0, 1) (i.e., clusters predominantly have the shape of a cylinder). For the system with salt, the main peak spreads and shifts toward regions of disks (0.5, 0.5) or spheres (1, 1), but morphologies are still very extended (flattened cylinders). All histograms (Figures 6 and 7) are rather wide both due to micelle shape and possible inaccuracy of cluster analysis method. It is quite difficult to distinguish a beltlike micelle from a few cylinders coming close to each other. On the basis of histograms (Figures 6 and 7) and on visual analysis of system snapshots (see Figure 4), we conclude that at a moderate salt concentration (C_1) the micelle shape is close to a cylinder, while increasing the salt concentration (C_2) leads to growth of flattened cylinders. The amount of cylindrical micelles with $N > 300$ in the system without inorganic salt is small, so we can easily determine them by cluster analysis and study their properties carefully (we observe one clearly distinguishable peak on the histograms). Upon increasing salt concentration to C_1 , the amount of micelles with $N > 300$ increases significantly, while a few long micelles could also join together due to inaccuracy of cluster analysis. At high salt concentration, cylindrical micelles become even more flat and curved, which is also reflected in the histograms of shape parameters (K_1, K_2).

Figure 8 shows the histograms of the maximum eigenvalue of the gyration tensor for systems with high (C_2) and moderate (C_1) salt concentration. For both cases, the maximum linear size of big clusters ($1500 < N < 2500$) is larger than that of middle-sized clusters ($300 < N < 800$). The difference between distributions of the parameter λ_1 for middle-sized and big clusters is more pronounced for higher salt concentration (see plots at the top). Distribution of the parameter λ_1/R_g^2 is almost the same (see plots at the bottom), which means that the shape of middle-sized and big clusters is the same (i.e., their sizes along all axes are proportionally different).

3.4. Size of Micelles. In Figure 9, we perform a qualitative comparison of simulation and experimental data, which allows us also to match the scales of model parameter C and inorganic salt concentration. The fraction of the number of clusters with the number of particles $N > 300$ for lecithin/bile salts (SC and SDC) mixtures as a function of inorganic salt concentration from computer simulation (Figure 9a) are compared with experimental data²² on zero-shear viscosity η_0 of the lecithin/bile salt mixtures in water (Figure 9b). In accordance with Figures 5 and 6, increasing of parameter C leads to increasing of

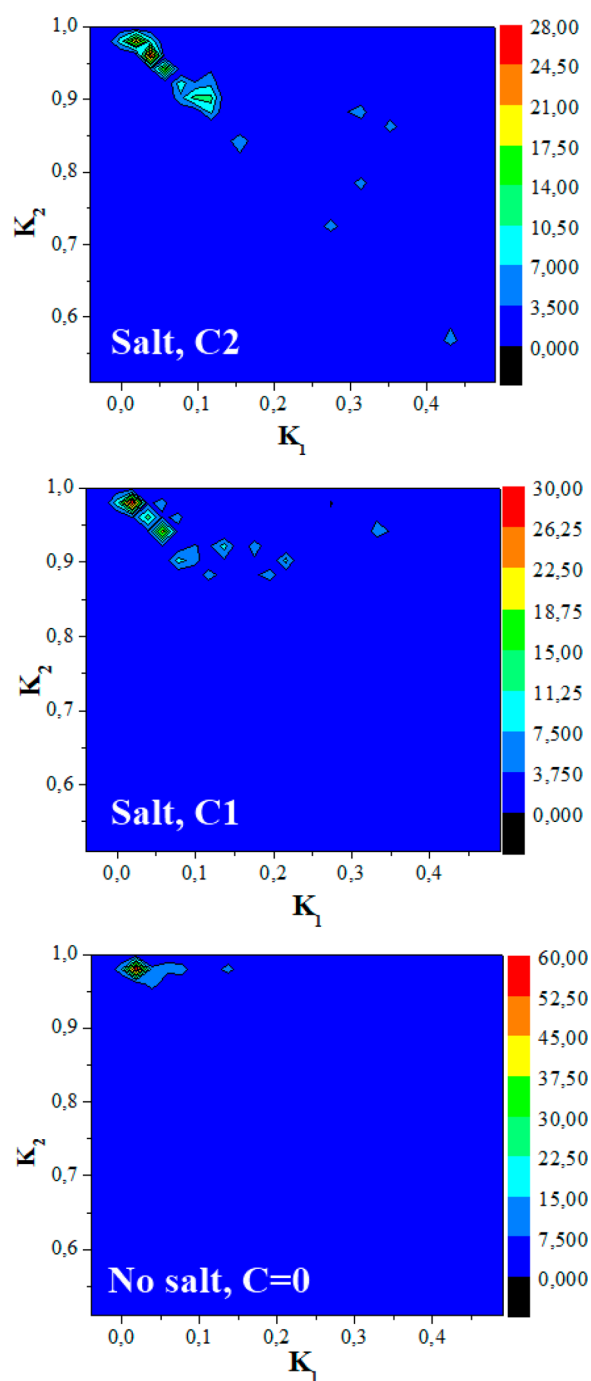


Figure 7. Two-dimensional histogram of (K_1, K_2) parameters for systems in the presence of inorganic salt with concentrations C_2 and C_1 and without salt $C = 0$ (from top to bottom) for clusters having the number of particles $N > 300$.

the amount of big micelles due to aggregation of small micelles. Adding of excess amount of salt $C > C_2$ may cause macrophase separation (e.g., we observe the formation of a single micelle at $C = 0.25$). The ends of the curves both for SC and SDC correspond to the salt concentrations above, which the samples undergo phase separation into two liquid phases. In the experiment, it corresponds to destruction of entanglements and precipitation. In ref 22, SC samples remained homogeneous until the NaCl concentration ~ 6 M was reached, while the macrophase separation for SDC was observed at a NaCl concentration of about 2.5 M. In our CG model, we also

observe that the SDC system undergoes macrophase separations at lower C values than SC. We have found that the number of big clusters increases up to 4 times for both systems shortly before separation. We do not measure the viscosity of our system due to restrictions of DPD method, but the number of big clusters and their length should play the key role in the viscosity increasing.

Within the framework of our CG model, with the chosen system size, we are not able to directly calculate entanglements in our system for several possible reasons: (1) visual analysis of the system in Figure 4 allows us to conclude that micelles are oriented predominantly almost parallel to each other and their length is not large enough to form entanglements; (2) simulation box size is still a smaller characteristic size where entanglements are expected to appear; and (3) simulation time is not sufficient to observe diffusion of micelles. Maybe we can overcome these limitations by increasing system size and simulation time, but at this moment, we do not observe real entanglements in our system, so we are not able to calculate viscosity parameters.

3.5. Growth Mechanism of Micelles. Structures formed in the aqueous solution of lecithin and bile salt are mainly affected by the low-molecular weight salt concentration. The shape of self-assembled structures is controlled by the effective geometry of the amphiphiles, which can be simply expressed by critical packing parameter (CPP), calculated as ratio of the volume of tails to composition of the headgroup area and the tail length.^{54,55} The values of CPP in the range from 1/3 to 1/2 correspond to the cylindrical micelles; increasing the CPP value up to 1 means formation of bilayers or vesicles. The lecithin molecules with a nearly cylindrical molecular shape ($CPP \sim 1$) prefer to assemble in the low-curvature bodies. Opposite, bile salt molecules tend to form highly curved small micelles with a low aggregation number. In the case of lecithin/bile salt mixture (without an inorganic salt), the effective packing parameter decreases down to 1/3–1/2 due to the incorporation of bile salt molecules between lecithin head groups (see Figure 10, left part, note also the change of the core in ellipsoidal micelles in comparison to vesicles). We can see that the phospholipid molecules are oriented radially. The bile salt molecules are situated at the surface of cylindrical micelles formed by phospholipid molecules and act as wedges between the phospholipid head groups, as it was also observed for the same systems in ref 15. The end-caps of the cylinders (or ellipsoids) consist preferably of the bile salt molecules due to their shape. The length of the micelles in this case is determined by the ratio between lecithin and bile salt molecules. Lecithin molecules are predominantly located in the low-curvature cylindrical bodies, while bile salts form the roundings at the ends. At low bile salt concentration, the amount of bile salts is insufficient to reduce CPP for forming cylinders. With increasing bile salt concentration, the number of cylindrical micelles increases, but their length is limited due to more end-caps formed by bile salts. Further increasing bile salt concentration causes the CPP values to further decrease, and thus the cylindrical micelles turn into shorter or even spherical ones. Therefore, the growth of wormlike micelles in lecithin/bile salt solution is observed only for a specific interval of values of the molar volume ratio.^{22,56–58}

The right part of Figure 10 schematically displays mechanism of the long structures formation. Low-molecular weight salt decreases solubility of polar groups of lecithin and bile salt in water. Growth from small micelles to large ones becomes more

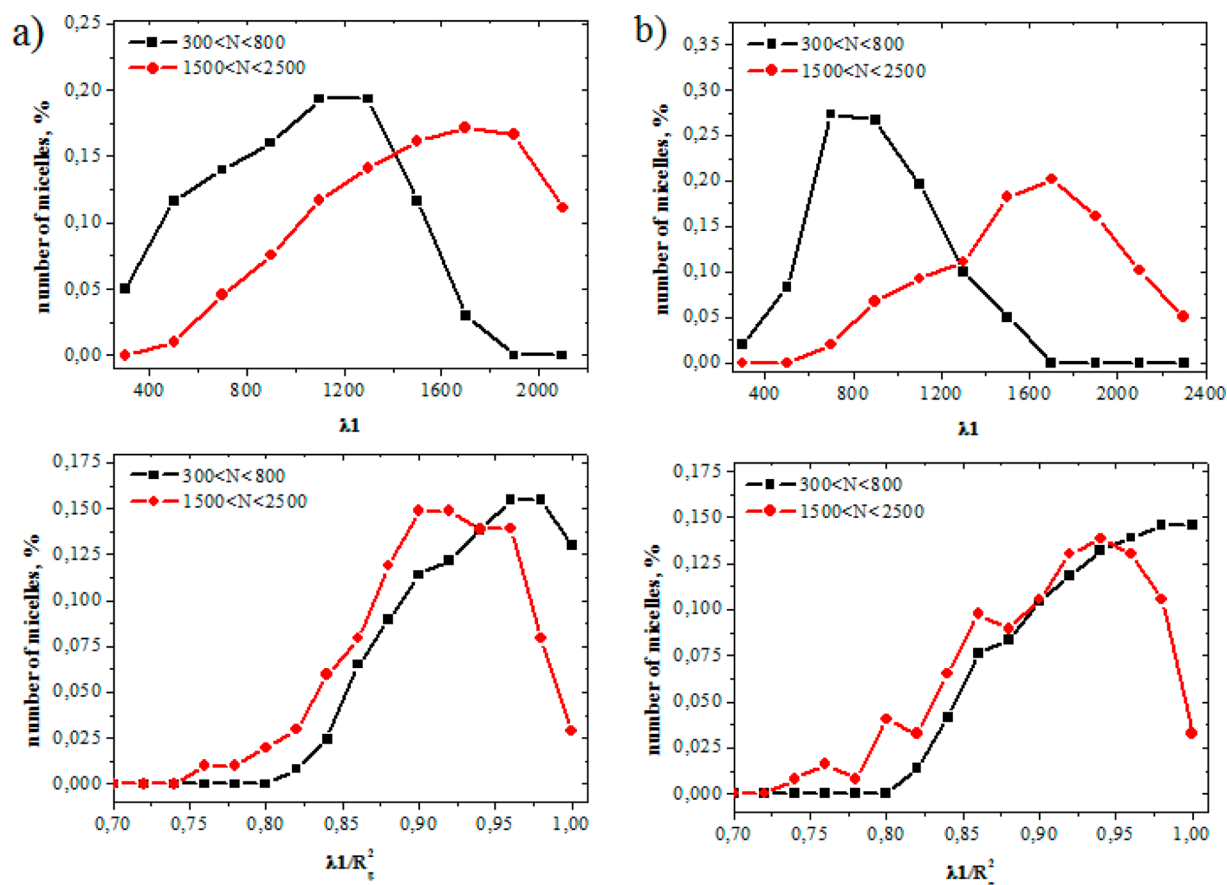


Figure 8. Histogram of the maximum eigenvalues of the inertia tensor (λ_1) (at the top) and normalized by the square gyration radius (at the bottom) for the salt concentration (a) C_1 and (b) C_2 . Black curves correspond to middle-sized clusters with the number of particles $300 < N < 800$ and red curves to big clusters with $1500 < N < 2500$.

favorable due to reducing the number of contacts of polar groups with water. The need for decreasing the effective surface of micelles causes the formation of highly elongated structures reminiscent of curved flattened cylinders (having elliptic cross-section). The further increasing of concentration of low-molecular weight salt leads to the macrophase separation since solubility of polar groups decreases significantly, and the micelles tend to minimize the number of contacts with water, form one big micelle, and precipitate. It may correspond to disappearance of gellike properties (i.e., the viscosity should decrease). This behavior is in good qualitative agreement with experimental data.²²

4. CONCLUSIONS

In this paper, we have improved the CG model for the lecithin/bile salt aqueous solution and applied the dissipative particle dynamics method to reveal the mechanism of experimentally observed²² viscosity increasing in such solutions upon the addition of inorganic salt. Growth of ellipsoidal structures in lecithin/bile salt mixture is due to the change of effective geometry of lecithin molecules (change of CPP value), while the addition of low-molecular weight salt leads to screening of electrostatic interactions between the polar groups and water. We have proposed a method to implicitly take into account the presence of inorganic salt in aqueous solution. In accordance with this method, the solubility of polar groups should be reduced upon increasing inorganic salt concentration, due to reducing the number of hydrogen bonds between the polar

groups of lecithin and bile salt and water (affinity of the polar groups to water) (i.e., we consider this factor to be the most important among several possible ones).

We have shown that upon increasing inorganic salt concentration, the number of large micelles, their volume fraction, and average size increase, and the rather short lecithin/bile salt micelles are transformed into wormlike structures. Such wormlike structures may entangle with each other and form a dynamic network, so that the solution behaves as a hydrogel. These results confirm the mechanism of viscosity increasing postulated in ref 22. The further increase of the inorganic salt concentration leads to the macrophase separation, which may correspond to the disappearance of experimentally observed gel-like properties. The shape of clusters having the number of particles $N > 300$ is cylinder-like; upon increasing inorganic salt concentration the micelles grow, and their shape is still close to a cylinder. At high salt concentration, we observe flattened cylinders, while middle-sized clusters with the number of particles $300 < N < 800$ and big clusters with $1500 < N < 2500$ have almost the same shape (but proportionally larger size). On the basis of the verified CG model, we can catch the main features of morphological changes in lecithin/bile salts mixtures both in organic solvents³³ and in water (in this paper). Results obtained by means of computer simulation in this paper and in ref 33 are in qualitative agreement with experimental results.^{22,23} This allows us to conclude that our model properly takes into account main features of real systems and is

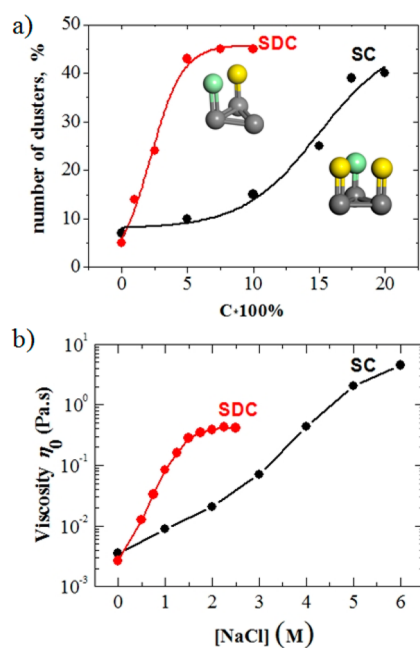


Figure 9. (a) Fraction of big clusters ($N > 300$) in the lecithin/bile salt mixtures (SC, black curve; SDC, red curve) as a function of parameter C obtained from computer simulation. (b) Experimentally obtained zero-shear viscosity η_0 of the lecithin/bile salt mixtures in water as a function of NaCl concentration. The lecithin concentration was fixed at 100 mM. The molar ratio of bile salt to lecithin B_0 of SC and SDC samples was 0.9 and 1.2, respectively.²²

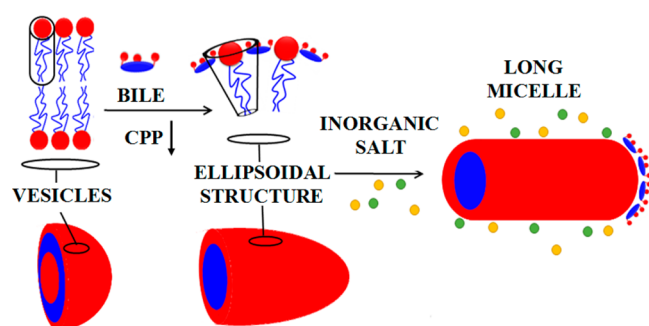


Figure 10. Growth mechanism of elongated micelles in the lecithin solution upon adding bile salt and inorganic salt.

appropriate for study of complex self-assembled structures²⁴ in lecithin/bile-salt systems.

We hope that our study brings new insight into the association behavior of lecithin/bile salt mixtures in aqueous solutions: (1) we have succeeded in developing new CG model working on larger time and length scales in comparison to previous simulations and allowing for the study of the evolution of many micelles; (2) we have studied the effect of inorganic salt; and (3) we have performed a comparison with the previous experiment.

AUTHOR INFORMATION

Corresponding Author

*E-mail: markina@polly.phys.msu.ru.

ORCID

Viktor A. Ivanov: 0000-0002-6581-3200

Pavel V. Komarov: 0000-0003-2138-5088

Shih-Huang Tung: 0000-0002-6787-4955

Notes

The authors declare no competing financial interest.

ACKNOWLEDGMENTS

This work was supported by the Russian Foundation for Basic Research (Grants 14-03-92004-NNS_a and 16-33-00294-mol_a) and the Ministry of Science and Technology of Taiwan (project 103-2923-E-002-005-MY3). We acknowledge useful discussions with Olga E. Philippova and Artem M. Romyantsev. We thank Moscow State University Supercomputer Center for providing the computational resources.⁵⁹

REFERENCES

- (1) Tamesue, N.; Inoue, T.; Juniper, K. Solubility of Cholesterol in Bile Salt-Lecithin Model Systems. *Am. J. Dig. Dis.* **1973**, *18* (8), 670–678.
- (2) Shrestha, H.; Bala, R.; Arora, S. Lipid-Based Drug Delivery Systems. *J. Pharm.* **2014**, *2014*, 1–10.
- (3) Hofmann, A. F.; Small, D. M. Detergent Properties of Bile Salts: Correlation with Physiological Function. *Annu. Rev. Med.* **1967**, *18*, 333–376.
- (4) Coello, A.; Meijide, F.; Nunez, E. R.; Tato, J. V. Aggregation Behavior of Bile Salts in Aqueous Solution. *J. Pharm. Sci.* **1996**, *85* (1), 9–15.
- (5) Palazzo, G. Wormlike Reverse Micelles. *Soft Matter* **2013**, *9*, 10668–10677.
- (6) Kreilgaard, M. Influence of Microemulsions on Cutaneous Drug Delivery. *Adv. Drug Delivery Rev.* **2002**, *54*, S77–98.
- (7) Byk, G. In *Pharmaceutical Perspectives of Nucleic Acid-based Therapy*; Mahato, R. I., Kim, S. W., Eds.; CRC Press, 2003; p 272.
- (8) Walker, S.; Sofia, M. J.; Kakarla, R.; Kogan, N. A.; Wierichs, L.; Longley, C. B.; Bruker, K.; Axelrod, H. R.; Midha, S.; Babu, S.; et al. Cationic Facial Amphiphiles: a Promising Class of Transfection Agents. *Proc. Natl. Acad. Sci. U. S. A.* **1996**, *93* (4), 1585–1590.
- (9) Faustino, C.; Serafim, C.; Rijo, P.; Reis, C.P. Bile Acids and Bile Acid Derivatives: Use in Drug Delivery. *Expert Opin. Drug Delivery* **2016**, *13* (8), 1133–1148.
- (10) Tu, K.; Tobias, D.; Klein, M. Constant Pressure and Temperature Molecular Dynamics Simulation of a Fully Hydrated Liquid Crystal Phase Dipalmitoylphosphatidylcholine Bilayer. *Biophys. J.* **1995**, *69* (6), 2558–2562.
- (11) Guo, X. D.; Zhang, L. J.; Wu, Z. M.; Qian, Y. Dissipative Particle Dynamics Studies on Microstructure of pH-Sensitive Micelles for Sustained Drug Delivery. *Macromolecules* **2010**, *43* (18), 7839–7844.
- (12) Huynh, L.; Perrot, N.; Beswick, V.; Rosilio, V.; Curmi, P.; Sanson, A.; Jamin, N. Structural Properties of POPC Monolayers under Lateral Compression: Computer Simulations Analysis. *Langmuir* **2014**, *30* (2), 564–573.
- (13) Holmboe, M.; Larsson, P.; Anwar, J.; Bergström, C. Partitioning into Colloidal Structures of Fasted State Intestinal Fluid Studied by Molecular Dynamics Simulations. *Langmuir* **2016**, *32* (18), 12732–12744.
- (14) Marrink, S.; Risselada, J.; Yefimov, S.; Tieleman, P.; de Vries, A. H. The MARTINI Force Field: Coarse Grained Model for Biomolecular Simulations. *J. Phys. Chem. B* **2007**, *111* (27), 7812–7824.
- (15) Marrink, S.; Mark, A. Molecular Dynamics Simulations of Mixed Micelles Modeling Human Bile. *Biochemistry* **2002**, *41* (17), 5375–5382.
- (16) Partay, L.; Jedlovsky, P.; Sega, M. Molecular Aggregates in Aqueous Solutions of Bile Acid Salts. Molecular Dynamics Simulation Study. *J. Phys. Chem. B* **2007**, *111* (33), 9886–9896.
- (17) Verde, A.; Frenkel, D. Simulation Study of Micelle Formation by Bile Salts. *Soft Matter* **2010**, *6*, 3815–3825.
- (18) Mögel, H.; Wahab, M.; Schmidt, R.; Schiller, P. Computer Simulation of Solubilization of Liposomes by Bile Salts. *Chem. Lett.* **2012**, *41* (10), 1066–1068.

- (19) Haustein, M.; Schiller, P.; Wahab, M.; Mögel, H. Computer Simulations of the Formation of Bile Salt Micelles and Bile Salt/DPPC Mixed Micelles in Aqueous Solutions. *J. Solution Chem.* **2014**, *43* (9–10), 1755–1770.
- (20) Haustein, M.; Wahab, M.; Mögel, H.; Schiller, P. Vesicle Solubilization by Bile Salts: Comparison of Macroscopic Theory and Simulation. *Langmuir* **2015**, *31* (14), 4078–4086.
- (21) Español, P.; Warren, P. Perspective: Dissipative Particle Dynamics. *J. Chem. Phys.* **2017**, *146* (15), 150901–150916.
- (22) Cheng, C.-Y.; Oh, H.; Wang, T.-Y.; Raghavan, S. R.; Tung, S.-H. Mixtures of Lecithin and Bile Salt Can Form Highly Viscous Wormlike Micellar Solutions in Water. *Langmuir* **2014**, *30* (34), 10221–10230.
- (23) Tung, S.-H.; Huang, Y.-E.; Raghavan, S. R. A New Reverse Wormlike Micellar System: Mixtures of Bile Salt and Lecithin in Organic Liquids. *J. Am. Chem. Soc.* **2006**, *128* (17), 5751–5756.
- (24) Wu, Z.; Yan, Y.; Huang, J. Advanced Molecular Self-Assemblies Facilitated by Simple Molecules. *Langmuir* **2014**, *30* (48), 14375–14384.
- (25) Lin, S.-T.; Lin, C.-S.; Chang, Y.-Y.; Whitten, A.; Sokolova, A.; Wu, C.-M.; Ivanov, V.; Khokhlov, A.; Tung, S.-H. Effects of Alkali Cations and Halide Anions on the Self-Assembly of Phosphatidylcholine in Oils. *Langmuir* **2016**, *32* (46), 12166–12174.
- (26) Lee, H.-Y.; Diehn, K.; Ko, S.; Tung, S.-H.; Raghavan, S. Can Simple Salts Influence Self-Assembly in Oil? Multivalent Cations as Efficient Gelators of Lecithin Organosols. *Langmuir* **2010**, *26* (17), 13831–13838.
- (27) Binder, H.; Zschornig, O. The Effect of Metal Cations on the Phase Behavior and Hydration Characteristics of Phospholipid Membranes. *Chem. Phys. Lipids* **2002**, *115* (1–2), 39–61.
- (28) Schubert, B. A.; Kaler, E. W.; Wagner, N. J. The Microstructure and Rheology of Mixed Cationic/Anionic Wormlike Micelles. *Langmuir* **2003**, *19* (10), 4079–4089.
- (29) Kolushcheva, S.; Friedman, J.; Angel, I.; Jelinek, R. Membrane Interactions and Metal Ion Effects on Bilayer Permeation of the Lipophilic Ion Modulator DP-109. *Biochemistry* **2005**, *44* (36), 12077–12085.
- (30) Baldwin, R. How Hofmeister Ion Interactions Affect Protein Stability. *Biophys. J.* **1996**, *71* (4), 2056–2063.
- (31) Lo Nostro, P.; Ninham, B. W. Hofmeister Phenomena: an Update on Ion Specificity in Biology. *Chem. Rev.* **2012**, *112* (4), 2286–2322.
- (32) Korchagina, E.; Philippova, O. Ion-Specific Self-Assembly of Hydrophobically Modified Polycation of Natural Origin. *Macromolecules* **2015**, *48* (23), 8622–8628.
- (33) Markina, A.; Ivanov, V.; Komarov, P.; Khokhlov, A.; Tung, S.-H. Self-Assembly of Micelles in Organic Solutions of Lecithin and Bile Salt: Mesoscale Computer Simulation. *Chem. Phys. Lett.* **2016**, *664*, 16–22.
- (34) Español, P.; Warren, P. Statistical Mechanics of Dissipative Particle Dynamics. *Europhys. Lett.* **1995**, *30* (4), 191–196.
- (35) Groot, R.; Warren, P. Dissipative Particle Dynamics: Bridging the Gap Between Atomistic and Mesoscopic Simulation. *J. Chem. Phys.* **1997**, *107* (11), 4423–4435.
- (36) Hildebrand, J. Solubility. XII. Regular Solutions. *J. Am. Chem. Soc.* **1929**, *51* (1), 66–80.
- (37) Hildebrand, J. Order from Chaos. *Science* **1965**, *150*, 441–450.
- (38) Groot, R.; Rabone, K. Mesoscopic Simulation of Cell Membrane Damage, Morphology Change and Rupture by Nonionic Surfactants. *Biophys. J.* **2001**, *81* (2), 725–736.
- (39) Srivastava, A.; Voth, G. Hybrid Approach for Highly Coarse-Grained Lipid Bilayer Models. *J. Chem. Theory Comput.* **2013**, *9* (1), 750–765.
- (40) Pattanayak, S.; Chowdhuri, S. Effect of Water on Solvation Structure and Dynamics of Ions in the Peptide Bond Environment: Importance of Hydrogen Bonding and Dynamics of the Solvents. *J. Phys. Chem. B* **2011**, *115* (45), 13241–13252.
- (41) Pattanayak, S.; Chowdhuri, S. A Molecular Dynamics Simulations Study on the Behavior of Liquid N-methylacetamide in Presence of NaCl: Structure, Dynamics and H-bond Properties. *J. Mol. Liq.* **2012**, *172*, 102–109.
- (42) Pattanayak, S.; Chowdhuri, S. Size Dependence of Solvation Structure and Dynamics of Ions in Liquid N-methylacetamide: A Molecular Dynamics Simulation Study. *J. Theor. Comput. Chem.* **2012**, *11* (02), 361–377.
- (43) Baburkin, P.; Komarov, P.; Khizhnyak, S.; Pakhomov, P. Simulation of Gelation Process in Cysteine–Silver Solution by Dissipative Particle Dynamics Method. *Colloid J.* **2015**, *77* (5), 561–570.
- (44) Manning, G. Limiting Laws and Counterion Condensation in Polyelectrolyte Solutions I. Colligative Properties. *J. Chem. Phys.* **1969**, *51*, 924–933.
- (45) Partay, L.; Segal, M.; Jedlovsky, P. M Morphology of Bile Salt Micelles as Studied by Computer Simulation Methods. *Langmuir* **2007**, *23* (24), 12322–12328.
- (46) Askadskii, A. A. *Computational Materials Science of Polymers*; Cambridge International Science Publishing, 2001.
- (47) Sun, H. Ab Initio Calculations and Force Field Development for Computer Simulation of Polysilanes. *Macromolecules* **1995**, *28* (3), 701–712.
- (48) Komarov, P.; Veselov, I.; Chu, P.; Khalatur, P.; Khokhlov, A. Atomistic and Mesoscale Simulation of Polymer Electrolyte Membranes Based on Sulfonated Poly(ether ether ketone). *Chem. Phys. Lett.* **2010**, *487* (4–6), 291–296.
- (49) Groot, R. Electrostatic Interactions in Dissipative Particle Dynamics—Simulation of Polyelectrolytes and Anionic Surfactants. *J. Chem. Phys.* **2003**, *118* (24), 11265–11277.
- (50) Magid, L. The Surfactant–Polyelectrolyte Analogy. *J. Phys. Chem. B* **1998**, *102* (21), 4064–4074.
- (51) Allen, M. P.; Tildesley, D. J. *Computer Simulation of Liquids*; Clarendon Press: Oxford, 1987.
- (52) Ivanov, V.; Paul, W.; Binder, K. Finite Chain Length Effects on the Coil-Globule Transition of Stiff-Chain Macromolecules: A Monte Carlo Simulation. *J. Chem. Phys.* **1998**, *109* (13), 5659–5669.
- (53) Khalatur, P. Effect of Volume Interactions on the Shape of a Polymer Coil. *Polym. Sci. U.S.S.R.* **1980**, *22* (10), 2438–2448.
- (54) Israelachvili, J.; Mitchell, D.; Ninham, B. Theory of Self-Assembly of Hydrocarbon Amphiphiles into Micelles and Bilayers. *J. Chem. Soc., Faraday Trans. 2* **1976**, *72*, 1525–1568.
- (55) Israelachvili, J. N. *Intermolecular and Surface Forces*, 3rd ed.; Academic Press: San Diego, 2011.
- (56) Madenci, D.; Salonen, A.; Schurtenberger, P.; Pedersen, J. S.; Egelhaaf, S. U. Simple Model for the Growth Behaviour of Mixed Lecithin-Bile Salt Micelles. *Phys. Chem. Chem. Phys.* **2011**, *13*, 3171–3178.
- (57) Gunnarsson, G.; Joensson, B.; Wennerstroem, H. Surfactant Association into Micelles. An Electrostatic Approach. *J. Phys. Chem.* **1980**, *84* (23), 3114–3121.
- (58) Akutsu, H.; Seelig, J. Interaction of Metal Ions with Phosphatidylcholine Bilayer Membranes. *Biochemistry* **1981**, *20* (26), 7366–7373.
- (59) Sadovnichy, V.; Tikhonravov, A.; Voevodin, V.; Opanasenko, V. *Contemporary High Performance Computing: From Petascale toward Exascale*; CRC Press: Boca Raton, 2013, p 283.